

CEBAF PROPOSAL COVER SHEET

This Proposal must be mailed to:

CEBAF
Scientific Director's Office
12000 Jefferson Avenue
Newport News, VA 23606

and received on or before OCTOBER 31, 1989

A. TITLE:

Coincidence Reaction Studies with the LAS

3. CONTACT PERSON:

L.B. Weinstein

ADDRESS, PHONE AND BITNET:

Massachusetts Institute of Technology - Laboratory for Nuclear Science
77 Massachusetts Avenue
Cambridge, MA 02139
Ph #: (617) 258-5438 Bitnet: WEINSTEIN@MITLNS

2. THIS PROPOSAL IS BASED ON A PREVIOUSLY SUBMITTED LETTER OF INTENT

YES
 NO

IF YES, TITLE OF PREVIOUSLY SUBMITTED LETTER OF INTENT

same as above

D. ATTACH A SEPARATE PAGE LISTING ALL COLLABORATION MEMBERS AND THEIR INSTITUTIONS

=====
(CEBAF USE ONLY)

Proposal Received 10-31-89

Log Number Assigned PR-89-027

By KES

contact: Weinstein

October 27, 1989

Dear members of the PAC,

At present the role of multinucleon absorption processes in deep inelastic electron scattering and the properties of the Δ resonance in nuclei are poorly understood and potentially very interesting and exciting subjects. The interest in this field is shown by the three CLAS experiments proposed to study various aspects of the (e,e') reaction mechanism.

- 'Coincidence Reaction Studies with the LAS' (spokesman: L. Weinstein, MIT) proposes to examine the various (e,e') reaction mechanisms in the quasielastic, dip, quasifree delta, and quasifree resonance regions at four beam energies from 600 to 2000 MeV with five targets from Deuterium to Lead.
- 'Study of Coincidence Reactions in the Dip and Delta-Resonance Regions' (spokesman: H. Baghaei, UMass) proposes to study the different processes that contribute to electron scattering in the dip and quasifree delta resonance regions and also to investigate the possible medium modifications of the Δ in nuclei at various energies with four targets from Helium to Lead.
- 'Electroexcitation of the $\Delta(1232)$ in the Nuclear Environment' (spokesman: R. Sealock, UVa) proposes to examine the position, width, and form factor of the delta resonance as a function of A , and Q^2 .

These experiments overlap significantly. They each intend to examine all reaction channels for a given (overlapping) set of electron kinematics. They will use similar targets, beam energies, luminosities, CLAS polarity, and triggering schemes. We expect that most of the data will be taken simultaneously, initially triggering data acquisition by detection of an electron so as to have an unbiased look at the hadronic final state. Later, we will use more selective triggers, that include hadronic requirements, to emphasize one or more aspects of these experiments. We plan to collaborate during the next few years on more thorough modeling of the CLAS acceptances and efficiencies as they affect these experiments so that we can optimize the various experimental plans.

Yours Sincerely,



Hossain Baghaei
Richard Sealock
Larry Weinstein

October 30, 1989

Coincidence Reaction Studies with the LAS

W. Bertozzi*, W. Boeglin*, S. Kowalski, L.B. Weinstein*
*Department of Physics and Laboratory for Nuclear Science
Massachusetts Institute of Technology*

V. Burkert, B. Mecking
Continuous Electron Beam Accelerator Facility

J.M. Finn, P.E. Ulmer
Department of Physics, The College of William and Mary

C.C. Chang, J.J. Kelly
Department of Physics, University of Maryland

R.W. Lourie, B. Norum
Department of Physics, University of Virginia

R. McKeown
Department of Physics, California Institute of Technology

* Co-spokesmen

ABSTRACT

We propose a series of survey experiments with the CLAS to determine the dominant channels that comprise the inclusive (e,e') response. For electron energy losses corresponding to the quasielastic peak, the dip region, Δ -resonance and higher N^* resonances, the response will be decomposed into $(e,e'p)$, $(e,e'n)$, $(e,e'd)$, $(e,e'pp)$, $(e,e'pn)$, $(e,e'p\pi)$ etc. Angular distributions of the various hadrons will be determined. Several targets, ranging from few-body systems up to heavy nuclei, will be examined. At the same time, we will try to separate the various nuclear response functions using the out-of-plane detection capabilities of the LAS.

I. Introduction and Motivation

The largest problem facing nuclear physics today is how to move beyond the simple independent-particle mean-field model of the nucleus. This model has worked well, but it only describes about 60% of the nuclear structure. In order to understand nuclear structure beyond this simple model of the nucleus, we must understand the higher order nuclear currents (eg: two-body, three-body ...). Our understanding of the reaction mechanisms (and hence of the currents) involved in deep inelastic electron scattering (quasielastic, dip, quasifree- Δ , and quasifree- N^*) from nuclei is poor. The CLAS provides a unique facility to investigate this question by allowing us to detect almost all of the particles emitted following virtual photon absorption. This will enable us to identify one-nucleon, two-nucleon, etc. knockout and isolate the contributions of the various nuclear currents to deep inelastic electron scattering.

We propose to carry out a set of broad survey experiments on the LAS involving the deuteron, ^3He or ^4He , ^{12}C or ^{16}O , ^{40}Ca , and Pb or U as representative nuclei of five regions of interest: the two-body system, few-body systems, light nuclei, medium nuclei, and large nuclear systems. We will detect all particles emitted by deep inelastic electron scattering. In addition to this basic survey, with the CLAS, we should be able to separate the various nuclear response functions (R_L, R_T, R_{LT}, R_{TT}) and determine the contributions to each response function of the various currents (one-body, two-body, etc.). We hope to separate the response functions for these reactions or at least to gain a qualitative understanding of these responses from comparing forward and backward angle spectra. This measurement will then provide a first experimental test of this capability.

These experiments are extensions of our present program at the Bates Linear Accelerator Center wherein we have been exploring the $^{12}\text{C}(e,e'p)$ reaction to help us understand anomalies with respect to one-body or mean field structure assumptions in (e,e') . Our Bates program is expanding to include a comprehensive measurement of the longitudinal, transverse, and interference structure functions of the deuteron, with and without polarized electrons. These new measurements will help us understand the $(e,e'p)$ process in the simplest real nucleus.

The anomalies observed in (e,e') include the enhanced transverse/longitudinal ratio in the quasielastic region, enhanced yields in the so called dip region and problems of yield and shape in the delta region. In our $^{12}\text{C}(e,e'p)$ work we explored the missing-energy structure in $(e,e'p)$ and the momentum transfer dependence of this structure. The kinematic selection of the reaction process via the (e,e') vertex, that is by the specification of (\vec{q}, ω) , is well established. Also, the existence of transverse two-body or many-body currents not contained in traditional independent nucleon assumptions has been demonstrated. There does not appear to be a strong reason to

invoke a $|\vec{q}|$ -dependent modification of nucleon transverse structure over the region of $|\vec{q}| < 1$ GeV/c or longitudinal structure for $|\vec{q}| < 600$ MeV/c.

These $^{12}\text{C}(e,e'p)$ experiments have all been carried out under the condition of parallel kinematics with two modest solid angle spectrometers and restricted for the most part to ^{12}C . It is our opinion that it will be very fruitful to undertake a broad survey to explore five regions of nuclear size and density. The CLAS will allow us to observe the distinctive and dominant quasifree processes: quasielastic scattering, quasifree delta excitation and quasi-free N^* excitation. We will also observe non-quasifree processes such as those already seen in our $^{12}\text{C}(e,e'p)$ work under the quasielastic peak, in the dip region and under the quasifree Δ peak. These non-quasifree processes include two-nucleon and many-nucleon knockout. Typical reactions detected will be $(e,e'N)$, $(e,e'N\pi)$, $(e,e'2N)$, $(e,e'3N)$, etc. This study should greatly clarify the role of multinucleon involvement in energy and momentum absorption. These are important reaction channels that are not understood in present theory. The CLAS provides a unique opportunity to directly observe these channels that up to now have merely been inferred.

There are many open questions in deep inelastic electron scattering that this series of experiments will try to answer. In the quasielastic region, $(e,e'p)$ experiments have consistently measured spectroscopic factors that are only 50–60% of the values expected from simple shell models.^{[1] [2] [3]} Where is the missing strength? Recent quasielastic $^{12}\text{C}(e,e'p)$ experiments at Bates in parallel kinematics at momentum transfers, q , of 585, 775, and 1000 MeV/c^[4] indicate that there is a very large cross-section stemming from two-or-more nucleon knockout ($\epsilon_m > 50$ MeV) (see figure 1). This non-one-body strength is 30 to 50% of the total $(e,e'p)$ yield in parallel kinematics at the peak of the quasielastic region. Below the quasielastic peak (see figure 1d), the non-one-body strength is much smaller. Various models indicate that strength at certain missing energies corresponds to two- or three- body knockout, but without detecting all final state particles we cannot be certain what the reaction mechanisms are. Furthermore, at present we have very limited data on the distribution of this strength in q and ω ; we have no data on the distribution of this strength except parallel to \vec{q} ; we have very limited data on the A dependence of this strength. This experiment will isolate and characterize the various components of these non-one-body currents and measure their q , ω , A , and angular dependences.

This experiment will also allow us to isolate the contribution from delta production at quasielastic kinematics. This contribution is frequently cited as being responsible for the difference in the transverse response function between theory and experiment. The quasielastic Bates missing energy spectra (figure 1a–c) show no increase in strength at pion threshold ($\epsilon_m = 160$ MeV), indicating that there is very little delta production at quasielastic kinematics. By detecting both the proton and the pion

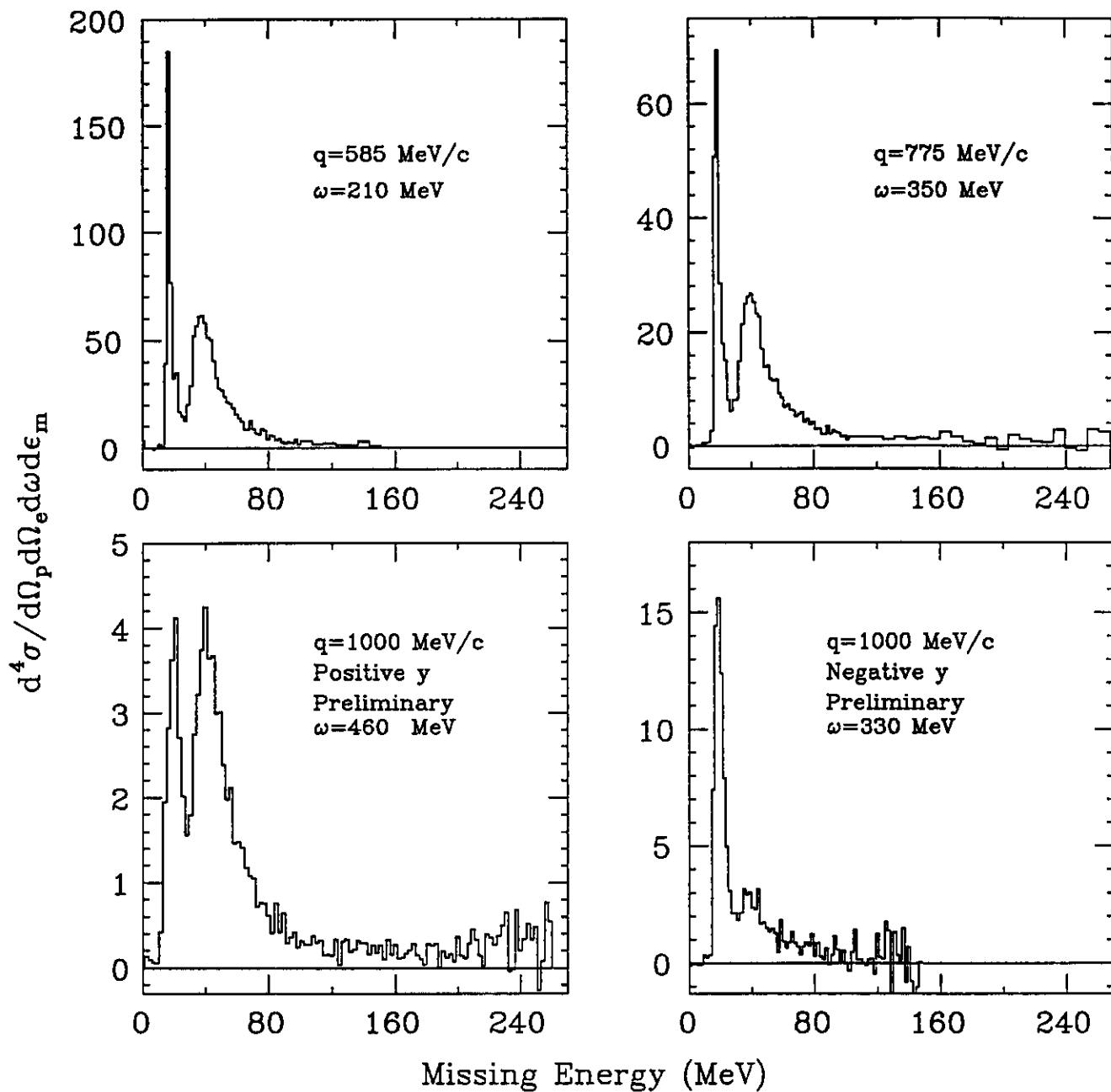


Figure 1. Missing energy spectra measured at the quasielastic peak at momentum transfers of a) 585 ($\omega = 210 \text{ MeV}$), b) 775 ($\omega = 350 \text{ MeV}$) and c) 1000 MeV/c ($\omega = 460 \text{ MeV}$). d) Missing energy spectrum measured on the low ω side of the quasielastic peak at $q = 1000 \text{ MeV}/c$ and $\omega = 315 \text{ MeV}$. The 1000 MeV/c data are preliminary.

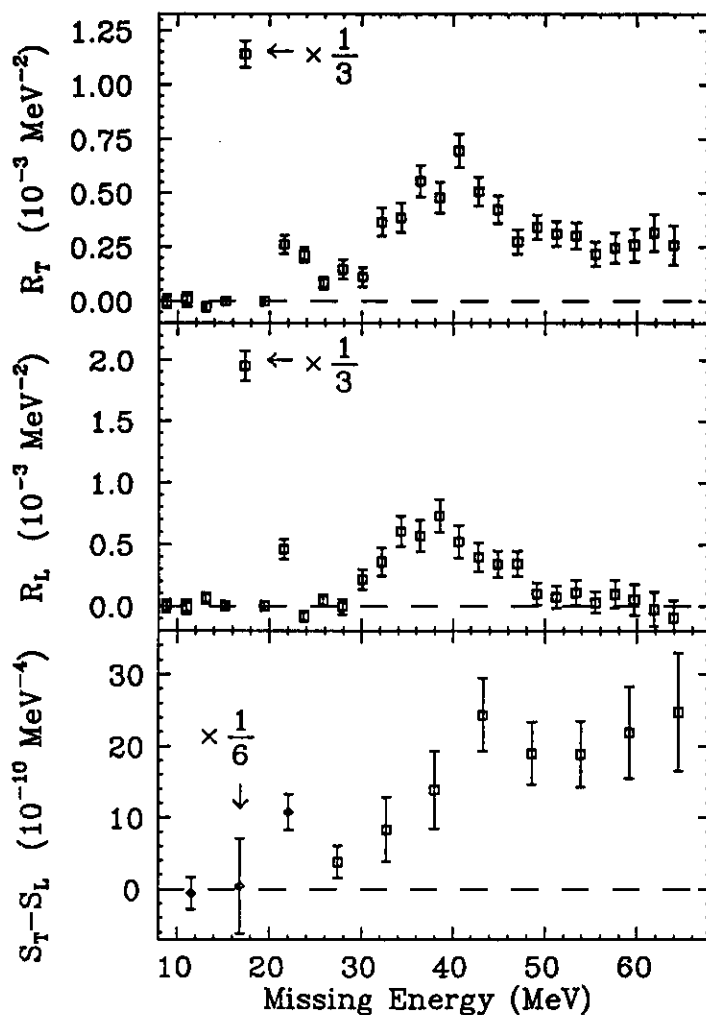


Figure 2. Separated $^{12}\text{C}(e,e'p)$ quasielastic response functions and their difference at $q = 400$ MeV/c and $\omega = 120$ MeV. Transverse (a) and longitudinal (b) response functions and difference in the spectral functions (c) vs. missing energy.

from delta decay, the CLAS will be able to unambiguously measure the contribution from delta production at quasielastic kinematics.

In the quasielastic region, we hope to distinguish between proton knockout from the s-shell and two particle knockout. These processes cannot be separated in $(e,e'p)$. Results from Bates (see figure 2) indicate that the excess transverse strength in the quasielastic region at $q = 400$ MeV/c is concentrated in the region of missing energy from 30 to above 65 MeV.^[5] This region contains both s-shell and two particle knockout. We expect s-shell proton knockout to be followed by isotropic low energy nucleon emission as the highly excited nucleus decays. We expect the low energy particle emitted in two nucleon knockout to be correlated in angle with the higher energy proton. S-shell knockout should be confined to the region of missing energy

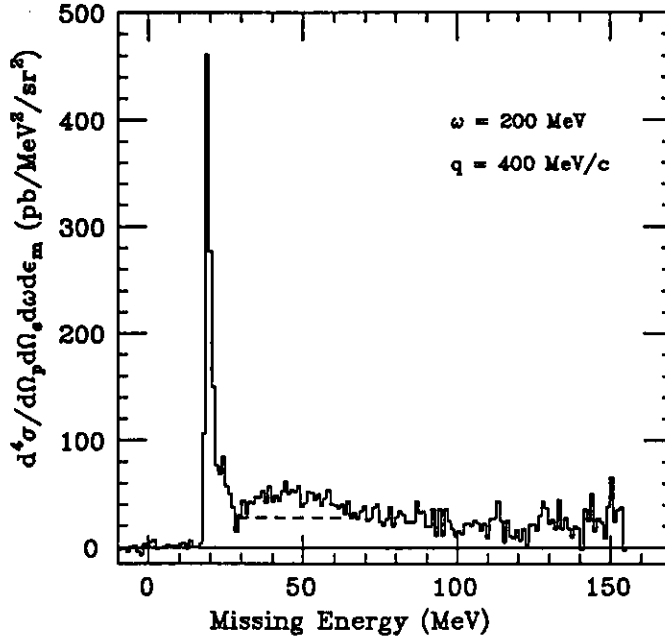


Figure 3. The missing energy spectrum from $^{12}\text{C}(e,e'p)$ in the dip region. The area above the dashed line is attributed to 1s proton knockout.

between 25 and 50 MeV; two or more nucleon knockout should extend to much higher missing energy. In a very low background environment we should be able to detect the low energy (5 – 10 MeV) neutrons emitted in such processes in the scintillator hodoscope with 5 – 10% efficiency. Low energy protons ($p_p < 200$ MeV/c) will not be detectable.

In the quasielastic region, we also do not understand the inclusive (e,e') longitudinal/transverse discrepancy. The $^{12}\text{C}(e,e')$ transverse response function is $\approx 60\%$ larger than the longitudinal.^{[6] [7]} Recent $^{12}\text{C}(e,e'p)$ coincidence measurements from Bates^[8] indicate that at least some of the discrepancy is due to a transverse non-one-body current beginning at a missing energy of 28 MeV. This transverse current may be similar to the non-one-body strength observed in our dip region measurement (see below). The longitudinal and transverse response functions have extremely different shapes. We should be able to qualitatively resolve differences this large between response functions. We would learn a great deal if we could separate response functions in this region.

In the dip region, we will measure particle multiplicities accompanying nucleon knockout. $^{12}\text{C}(e,e'p)$ results from Bates (see figure 3) show that the $^{12}\text{C}(e,e'p)$ missing energy spectrum has a large flat continuum extending out to the highest missing energy measured.^[9] This continuum strength might be enough to explain the anomalous (e,e') dip region cross-section. Recent theoretical calculations by J.M. Laget^[10] and by T. Takaki^[11] indicate that two particle knockout cannot contribute to this cross-section above 80 MeV of missing energy. Takaki has shown that three

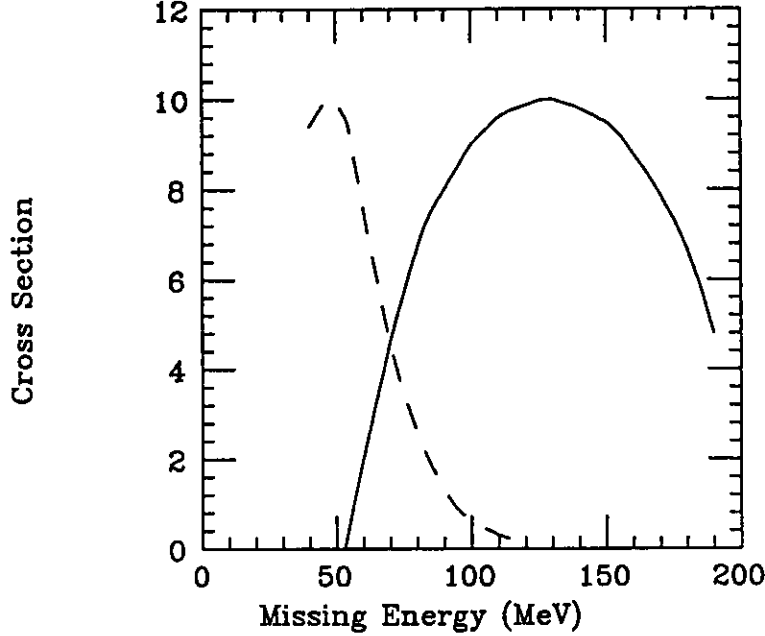


Figure 4. Missing energy spectra in the dip region for simple (arbitrarily normalized) models. Dashed curve: two nucleon absorption (zero range). Solid curve: three nucleon absorption (zero range).

nucleon processes can contribute in the range from 80 to 200 MeV of missing energy (see figure 4). The CLAS will allow us to unambiguously identify reaction channels that can only be inferred from current data. The dip region processes are primarily transverse. Measuring the dominant reaction mechanisms for the dip region will elucidate a currently poorly understood reaction channel.

In the region of the nucleon resonances, we will measure particle multiplicities accompanying nucleon knockout. In our $^{12}\text{C}(e,e'p)$ delta region experiments at Bates (see figure 5) we observed what appeared to be multinucleon knockout below pion threshold ($E_{miss} = 160$ MeV) and quasifree Δ knockout above pion threshold.^[12] We are currently unable to determine whether multinucleon knockout contributes in the region above pion threshold and how many nucleons are involved in the reaction.

The tagged photon coincidence studies by Kanazawa *et alia*^[13] on the deuteron and ^9Be imply that multinucleon knockout does contribute in the region above pion threshold. Two or more nucleon knockout (as indicated by the strength of the (γ_T, pn) cross-section in figure 5) dominates the region below pion threshold and extends beyond pion threshold. The large increase in yield at pion threshold is accompanied by real pion production (as indicated by the strength of the $(\gamma_T, p\pi)$ cross-section) presumably from Δ -production. Note that the (γ_T, pn) cross-section extends under the large peak to the lowest proton momenta indicating that $^{12}\text{C}(e,e'p)$ multiparticle knockout might similarly extend to the highest missing energies. These

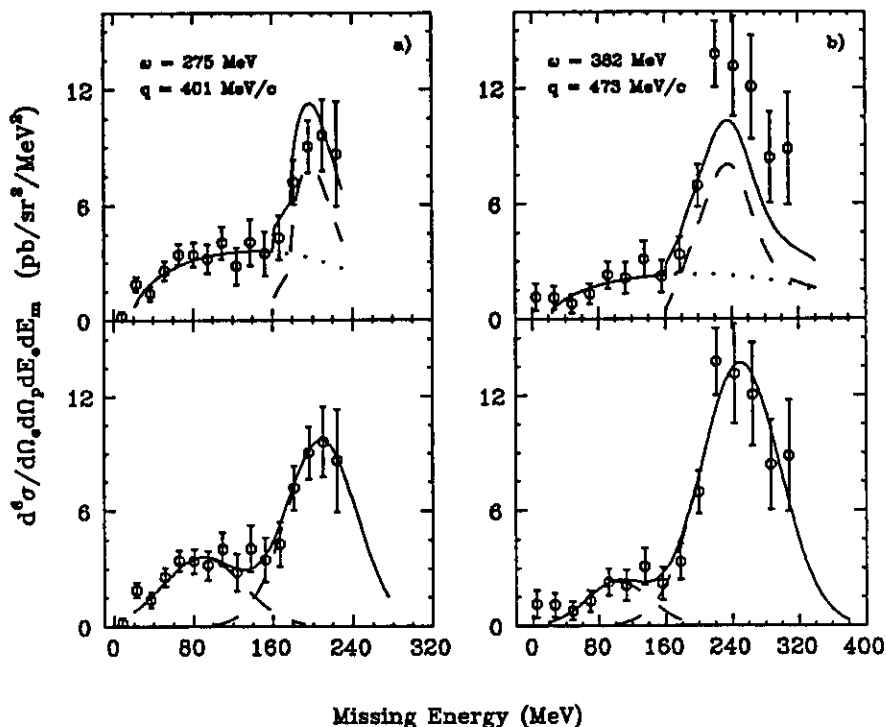


Figure 5. Missing energy spectra obtained in the region of the Δ resonance. The left spectra correspond to a point approximately halfway between the dip region and the Δ peak while the right spectra are at the maximum of the peak. In the upper figures the dashed curves are from a quasifree Δ -production calculation, the dotted curves are a three-body phase-space fit to the data, and the solid curves are the sum. The curves in the lower figures are Gaussian fits.

reactions are also primarily transverse. Detecting all of the particles knocked out will allow us to unambiguously separate the various reaction mechanisms.

Since we will automatically measure both forward and backward electrons as well as protons emitted at all angles with respect to the electron, we should be able to separate the various nuclear response functions, R_L , R_T , R_{LT} and R_{TT} . Although the moderate resolution of the CLAS will not allow us to perform few percent measurement of these separated responses we will be able to identify the dominant behavior of these response functions. We expect that the very large angular acceptances of the CLAS combined with the moderate momentum and angular resolutions will allow us to perform these separations.

For these preliminary experiments, we are interested in examining a few representative nuclei including the deuteron, $^3\text{He}/^4\text{He}$, ^{12}C or ^{16}O , ^{40}Ca , and Pb or U. Measuring the deuteron will allow us to characterize the (e,e') response in the simplest real nucleus. Measuring ^3He or ^4He will provide a good characterization of the (e,e') response in the few body system where such many-body phenomena as expressed in the dip region are relatively small. Measuring a light nucleus such as ^{12}C will connect with our series of measurements on ^{12}C performed at Bates. The

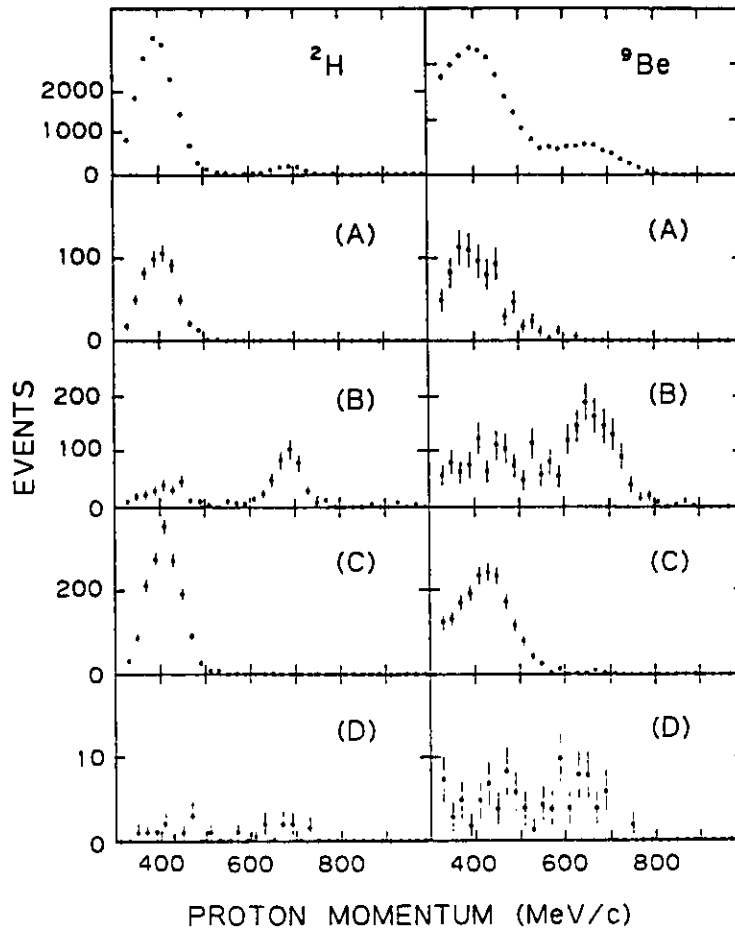


Figure 6. Tagged photon coincidence studies on ${}^9\text{Be}$ (right) and the deuteron (left). From top to bottom the reactions are (γ_T, p) , $(\gamma_T, p\gamma)$, (γ_T, pn) , $(\gamma_T, p\pi)$, and (γ_T, pp) . The figures show the distribution of final proton momentum for protons detected in coincidence with the specified second particle.

change in the relative strengths of different reaction mechanisms from Deuterium to Helium to Carbon should provide a stringent test of nuclear models. Measuring Calcium will allow us to explore a medium size nucleus. Measuring a heavy nucleus such as Lead will be the closest we can come to performing these experiments on the unattainable nuclear matter so dear to theorists' hearts.

We want to measure these reactions at beam energies of approximately 600, 1000, 1500 and 2000 MeV. The exact energies should be chosen to provide maximum compatibility with other experiments running simultaneously (eg: in Hall A). The 600 MeV measurement will tie in to existing work performed at Bates and other laboratories and will allow us to learn to operate the CLAS at energies where reaction mechanisms are more familiar and particle identification is easy. The experience gained at 600 MeV should facilitate running at higher energies. The 600 and 1000

MeV measurements taken together will provide data for attempting longitudinal-transverse response function separations at momentum transfers in the region of 600 to 1000 MeV/c. The higher energy data should provide separations at higher momentum transfers. The higher energy measurements will allow us to attain higher momentum and energy transfers and will provide a complete characterization of how the different reaction mechanisms change with momentum and energy transfer.

II. Experimental Technique

We will use the CLAS with a luminosity of about $10^{34} \frac{\text{nucleons} \times \text{electrons}}{\text{cm}^{-2} \text{sec}^{-1}}$ and we anticipate $< 1\%$ momentum resolution for electrons, protons, pions and other charged particles. The count rate estimates assume that the azimuthal coverage is 50% at 10° , 65% from 20 to 80° , and 85% at 90° .

We also anticipate a capability for neutron detection at the 5–10% efficiency level over a large portion of the solid angle of the LAS. We expect that there will be Čerenkov counter coverage from 0 to 45° in all segments and from 0 to 90° in one segment. This Čerenkov coverage is crucial to the experiment.

Unlike ‘standard’ magnetic spectrometer experiments, there are only three hardware variables associated with a CLAS experiment: beam energy, target, and triggering scheme.

The initial targets will be Deuterium, Helium, Carbon, Calcium, and Lead as representatives of the two body system, few body systems, light nuclei, medium nuclei, and heavy nuclei respectively.

As in every experiment, we will choose the trigger to minimize background while retaining as many of the ‘interesting’ events as possible. Proper triggering is more difficult for the CLAS than for a traditional magnetic spectrometer experiment since background cannot be eliminated by choice of magnetic spectrometer angles and fields. For the CLAS the detector background is fixed by the choice of beam energy, luminosity and target nucleus. Since computer data acquisition rates (10^2 – 10^3 Hz) are significantly lower than detector rates (10^6 Hz), we can choose the highest luminosity the detectors can tolerate (eg: $10^{34} \text{s}^{-1} \text{cm}^{-2}$), and choose a suitably restrictive hardware trigger so that we only look at ‘interesting’ events. In the current CLAS configuration, we will be able to make fast trigger decisions using Čerenkov counter information, scintillator hodoscope data, and crude momentum determinations from the drift chambers. Initially, while we are still learning about the CLAS, we will want to use as unrestrictive a trigger as possible so that we can study the CLAS characteristics offline. This limitation should not be a problem in the early days of the CLAS when we expect that almost everything will be interesting.

We want to eliminate elastic scattering events. We can do this by either requiring two detected particles or by cutting on the energy of the final electron. If we require two detected particles, then we are throwing away data about the hadron detection efficiencies of the CLAS. If we cut on the final electron energy, we will have to eliminate both the highest energy electrons from elastic scattering and the lowest energy electrons from the radiative tail. At small angles ($\theta_e < 30^\circ$) elastic scattering (including the radiative tail) completely dominates the cross-section at all ω . At these angles we will need to require a second particle in coincidence with the electron. At larger angles where elastic scattering is much smaller, we will want to cut only the highest and lowest energy electrons.

We also want to acquire the same number of events for different processes (so that we don't measure process A to 0.1% statistical error and process B to 10% statistical error). We will even out the data acquisition rate by sampling a prescaled fraction of electron scattering at different angles based on their frequency of occurrence. For example, if the cross-section for 30° deep inelastic electron scattering is 500 times greater than that for 90° scattering, we would acquire only 0.2% of the 30° events and all of the 90° events. A threshold Čerenkov counter is crucial to this experiment.

We propose to use electron beam energies of 600, 1000, 1500, and 2000 MeV. Starting our measurements at 600 MeV and working up to 2000 MeV will allow us to develop expertise in particle identification in successively harder regimes.

III. Counting Rates

Current $^{12}\text{C}(e,e'p)$ experiments at MIT-Bates utilize a luminosity of approximately $10^{36} \text{ s}^{-1} \text{ cm}^{-2}$ with spectrometer acceptances of approximately 0.01 sr and 10% $\frac{\Delta p}{p}$. The CLAS will have a maximum luminosity of $10^{34} \frac{\text{nucleons} \times \text{electrons}}{\text{cm}^{-2} \text{ sec}^{-1}}$ with approximately 2π sr and 100% $\frac{\Delta p}{p}$. The much greater acceptances of the CLAS will compensate for the reduced luminosity both by permitting measurement of many reactions at the same time and by permitting measurement of specific reactions much more efficiently.

The cross-sections for these kinematics are large. Figures 7 through 10 show the expected $^{12}\text{C}(e,e')$ cross-sections (in nb/MeV-sr) for these beam energies and angles. The cross-sections were computed using the program QFS by J. O'Connell and J. Lightbody. The solid lines show the total cross-section in nb/MeV-sr (not including the elastic radiative tail) at each energy and each angle as a function of electron energy loss. The dashed lines the contributions to this cross-section from quasielastic, two-nucleon, delta, and x-scaling processes. We expect that the cross-sections per nucleon should be A independent for quasifree processes. Figures 11 and 12 are the same as figures 7 and 9 with the inclusion of the elastic radiative tail. The upper solid line shows the cross-section including the radiative tail, the lower solid line

shows the inelastic cross-section only. Note that for $E_o = 600$ MeV, the radiative tail dominates the cross-section for small angles. At large angles and at $E_o = 1500$ MeV the radiative tail is small (although not negligible).

The counting rates for these kinematics are also large. Figures 7–10 show the expected counting rate per second per MeV for each beam energy and each angle (for a 10° bin in scattering angle). At 600 MeV and 90° , the total (e, e') counting rate is ≈ 20 per second (in a 10° bin). If the data acquisition rate is 300 events per second, then we will want to acquire 30 events per second per 10° bin. At 600 MeV, we will acquire all of the events for $\theta_e \geq 70^\circ$ and a prescaled fraction of events at smaller angles. At 1000 MeV, we will acquire all of the events for $\theta_e \geq 60^\circ$ and a prescaled fraction of events at smaller angles. At 1500 MeV, we will acquire all of the events for $\theta_e \geq 50^\circ$ and a prescaled fraction of events at smaller angles. We will be count rate limited for $\theta_e \geq 60^\circ$. At 2000 MeV, we will acquire all of the events for $\theta_e \geq 50^\circ$ and a prescaled fraction of events at smaller angles. We will be count rate limited for $\theta_e \geq 60^\circ$.

This experiment will cover such a wide range of kinematics and reactions that detailed simulation of detector efficiencies over the whole range of experimental conditions would be extremely time consuming. In addition to modeling the many single-particle-knockout reactions (which are moderately well understood) we would also have to model the multi-particle reactions (which are not understood). Before performing the experiment, we will model the various reactions as extensively as possible. Due to the wide range of kinematical situations and the survey nature of the experiment, we can use average CLAS efficiencies as a first approximation. Charged hadron detection efficiency will be a function of scattering angle. It will range from 50% at 10° to 85% at 90° . Therefore the average efficiency to detect one charged hadron will be $\approx 70\%$ and the average efficiency to detect two charged hadrons will be $\approx 50\%$. Neutron detection efficiencies will be about 5-10%.

Except at large angles and energies, the primary limitation on the event rate will come from the data acquisition system, not from the CLAS itself. Therefore, it is important to maximize the data acquisition rate. In our opinion, a data acquisition rate of 10^3 /sec is highly desirable; a rate of only 10^2 /sec will increase the beam time requirements for many interesting experiments. A rate of 10^3 per second is attainable with present technology.

We assume here that the data acquisition system will be able to acquire 300 events per second or 10^6 events per hour. We plan to bin the data in relatively coarse bins for the initial series of experiments (see table 1). We will bin the scattering angle into 10° bins. This is approximately the same as in our magnetic spectrometer experiments. We will bin the electron energy loss, ω , into 30 to 60 MeV bins (30 MeV at $E_o = 600$ MeV, 60 MeV at $E_o = 2000$ MeV). This will allow us to specify the

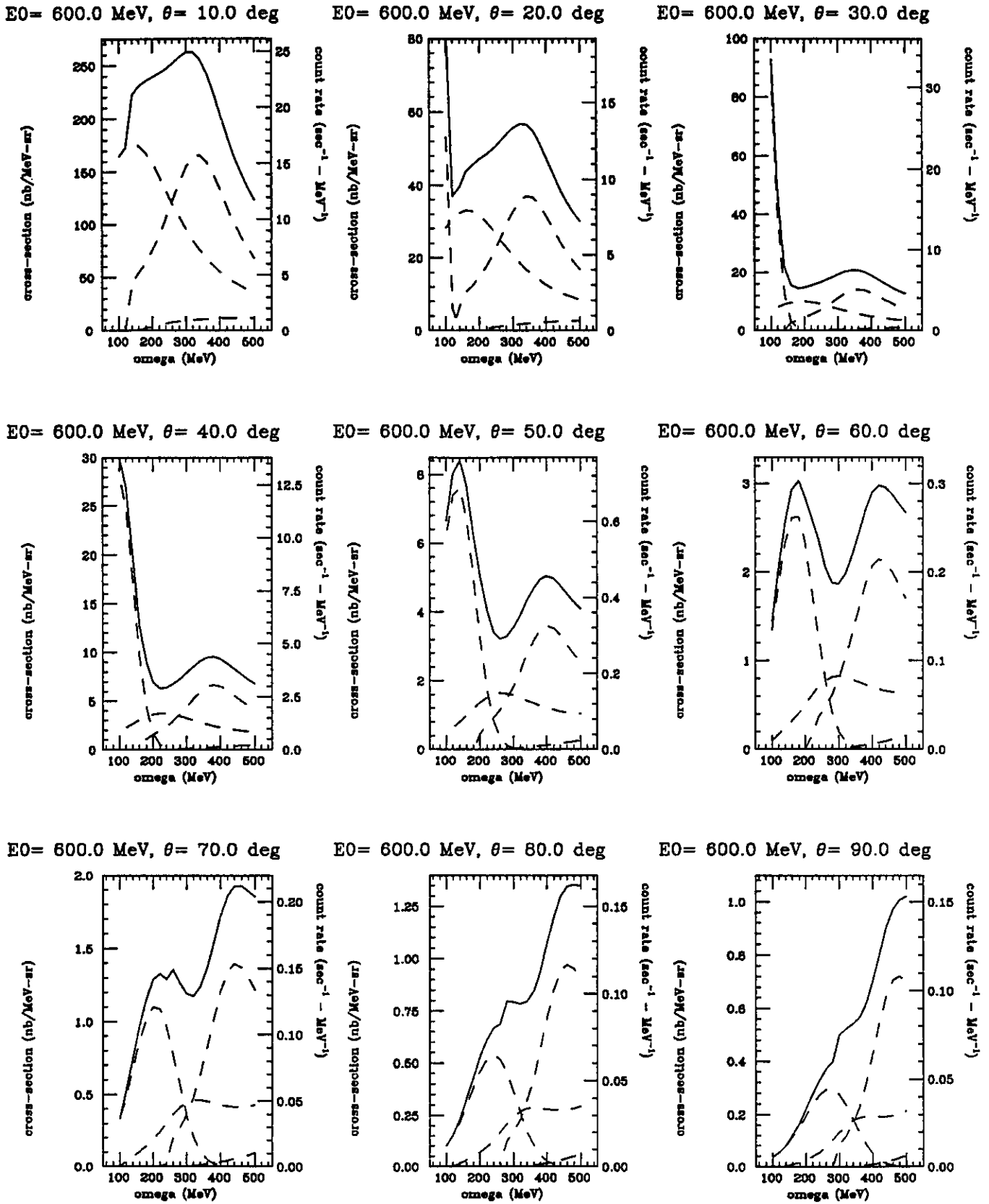
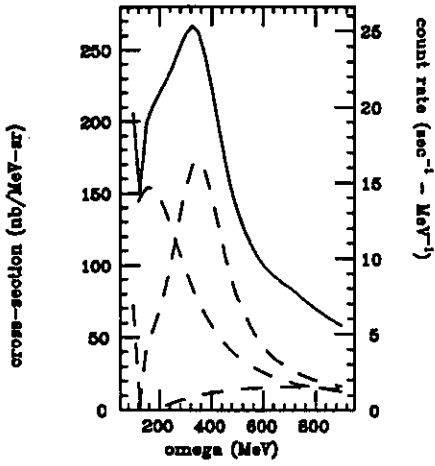
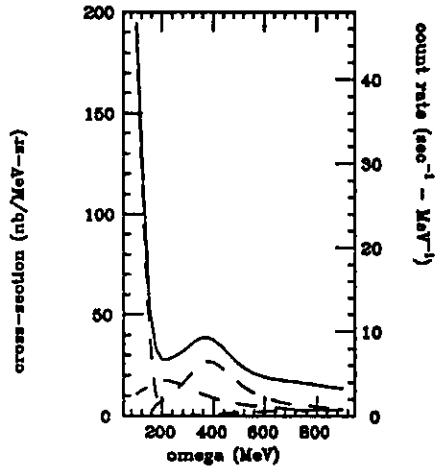


Figure 7. $E_0 = 600 \text{ MeV}$ CLAS cross-sections and counting rates. Elastic radiative tail not included.

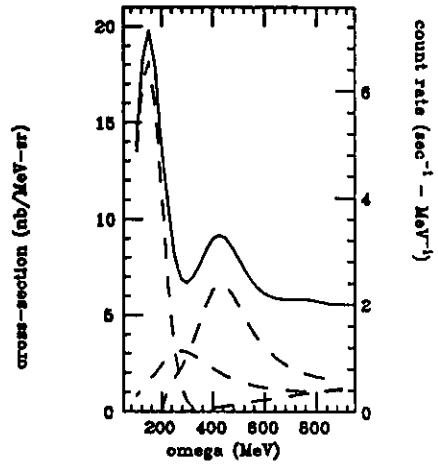
$E_0=1000.0$ MeV, $\theta= 10.0$ deg



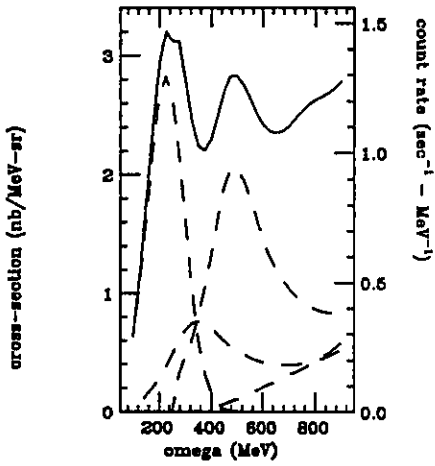
$E_0=1000.0$ MeV, $\theta= 20.0$ deg



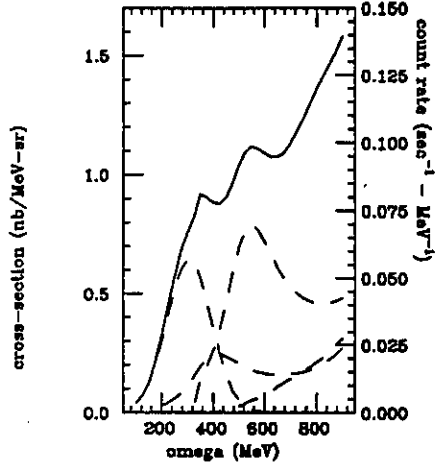
$E_0=1000.0$ MeV, $\theta= 30.0$ deg



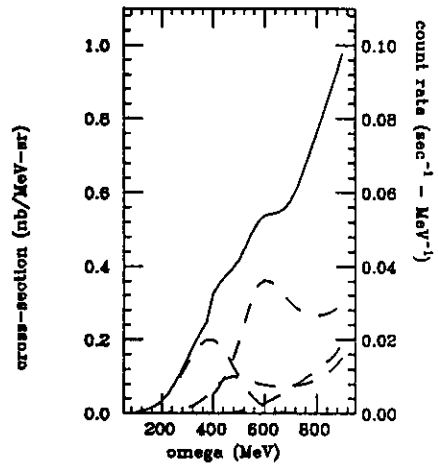
$E_0=1000.0$ MeV, $\theta= 40.0$ deg



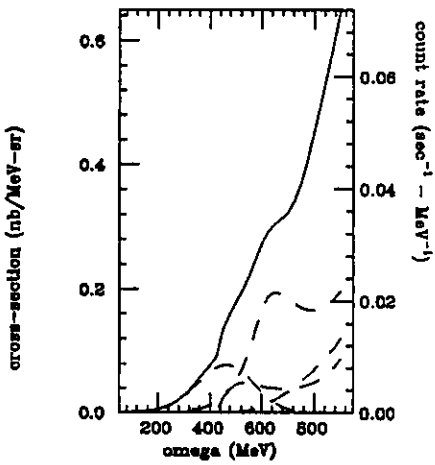
$E_0=1000.0$ MeV, $\theta= 50.0$ deg



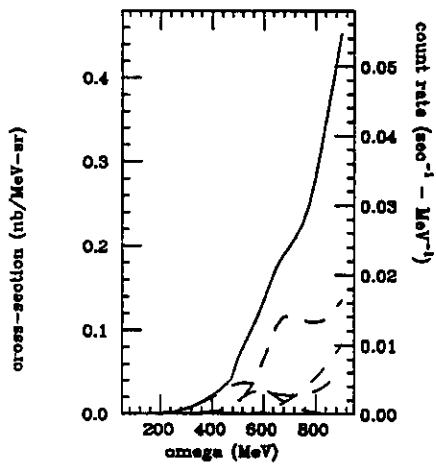
$E_0=1000.0$ MeV, $\theta= 60.0$ deg



$E_0=1000.0$ MeV, $\theta= 70.0$ deg



$E_0=1000.0$ MeV, $\theta= 80.0$ deg



$E_0=1000.0$ MeV, $\theta= 90.0$ deg

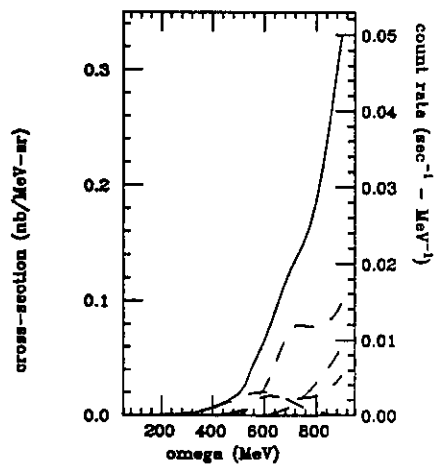


Figure 8. $E_0 = 1000$ MeV CLAS cross-sections and counting rates. Elastic radiative tail not included.

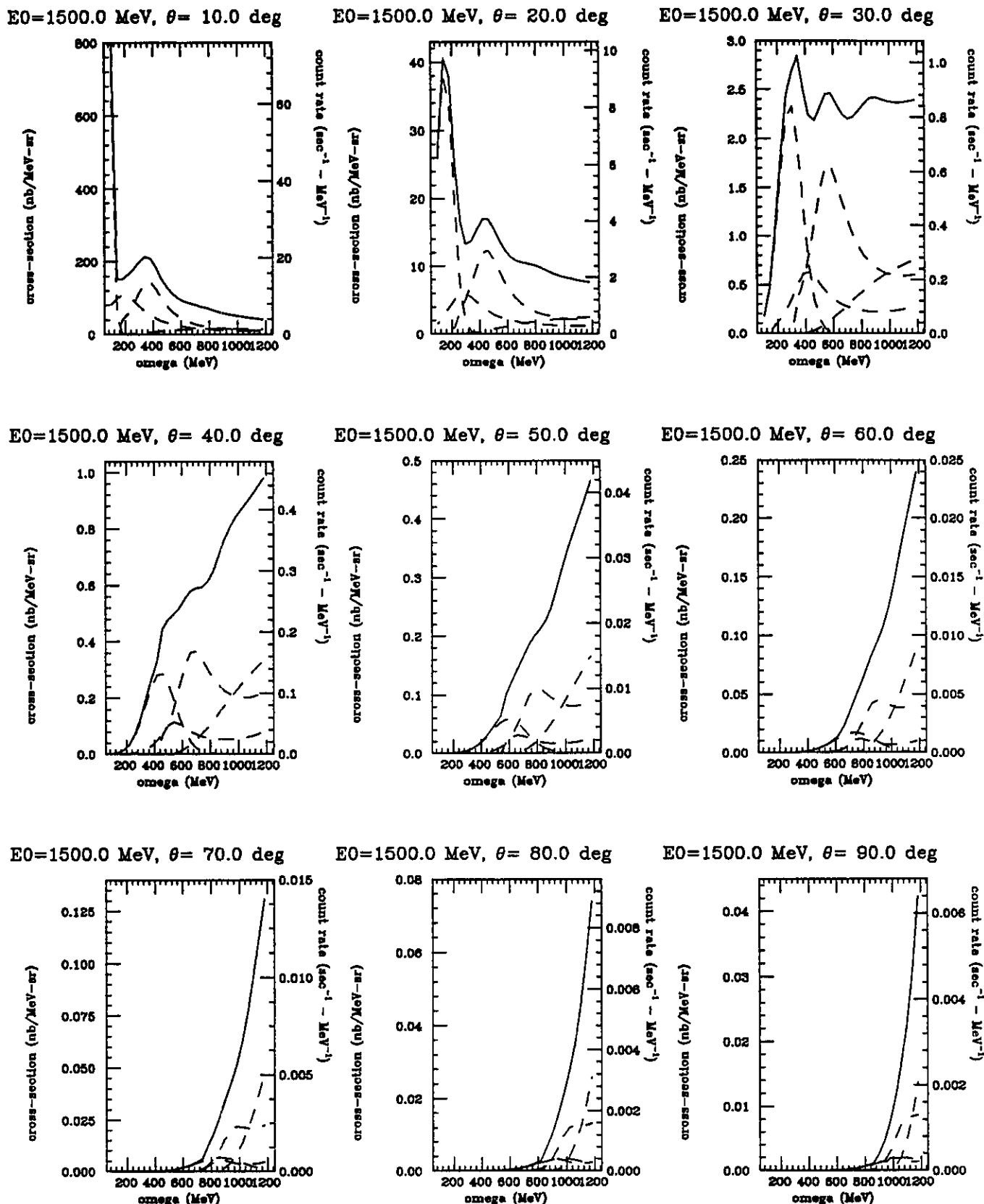


Figure 9. $E_0 = 1500$ MeV CLAS cross-sections and counting rates. Elastic radiative tail not included.

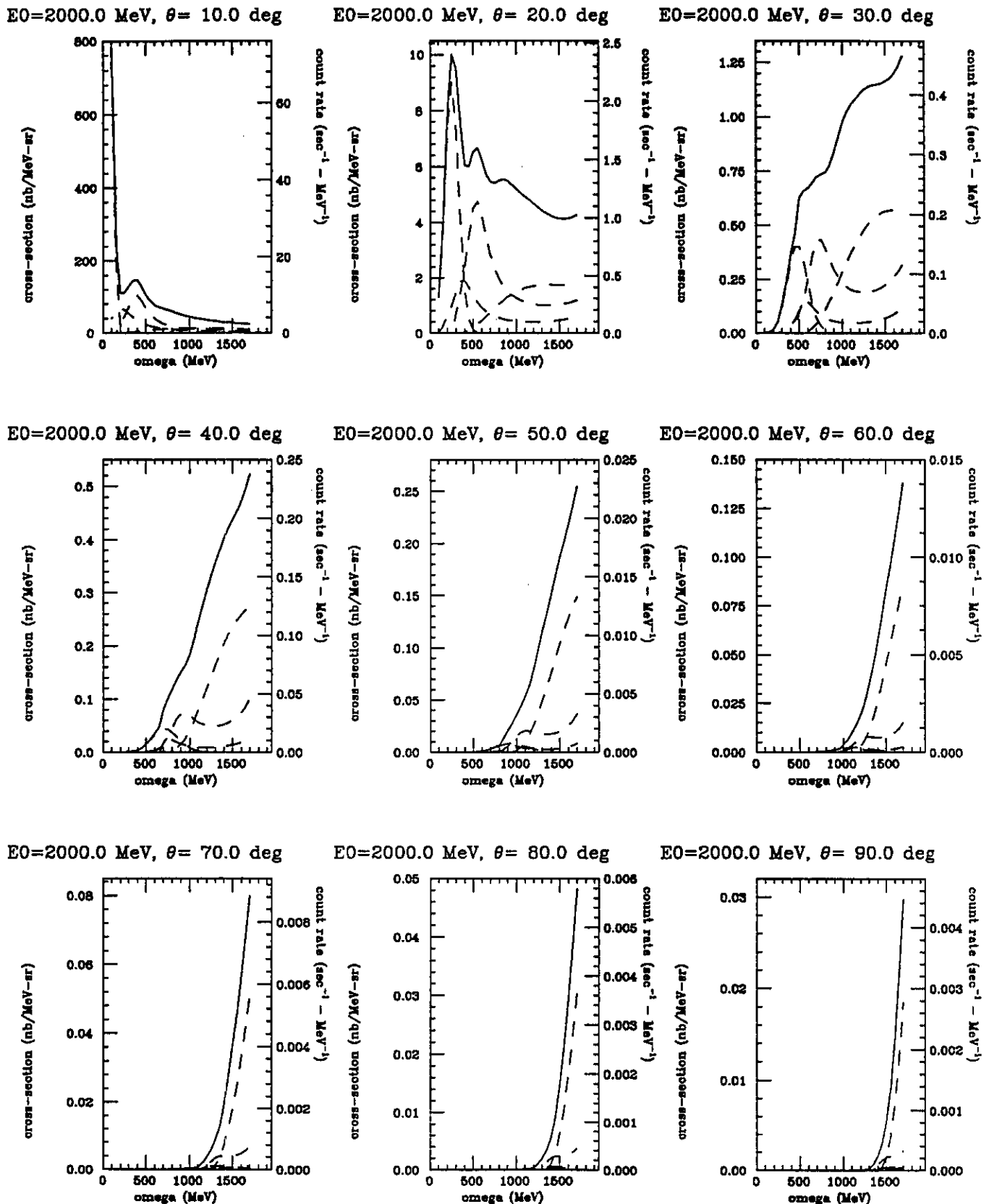
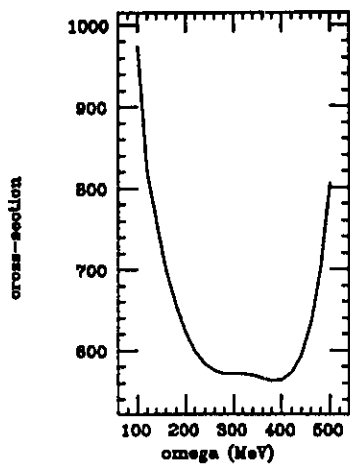
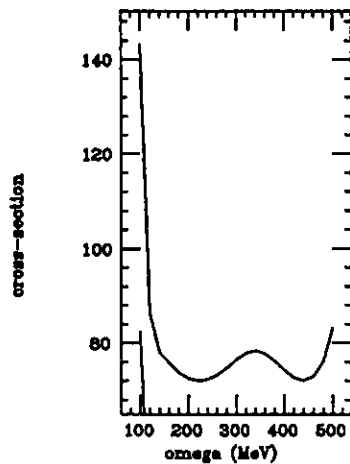


Figure 10. $E_0 = 2000$ MeV CLAS cross-sections and counting rates. Elastic radiative tail not included.

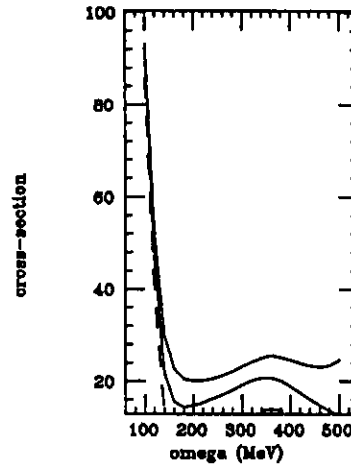
$E_0 = 600.0$ MeV, $\theta = 10.0$ deg



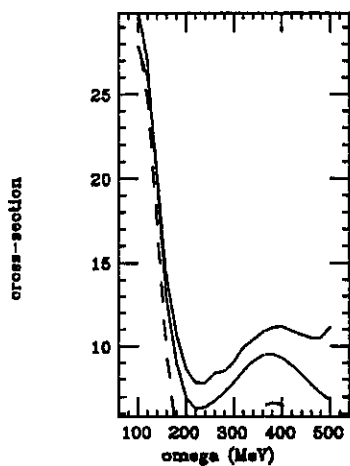
$E_0 = 600.0$ MeV, $\theta = 20.0$ deg



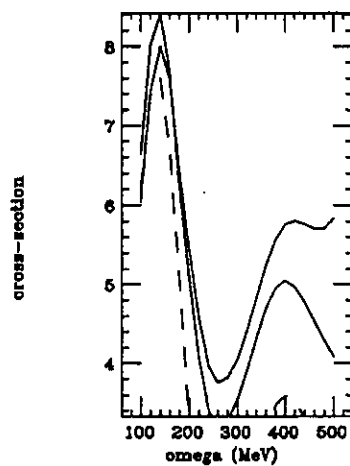
$E_0 = 600.0$ MeV, $\theta = 30.0$ deg



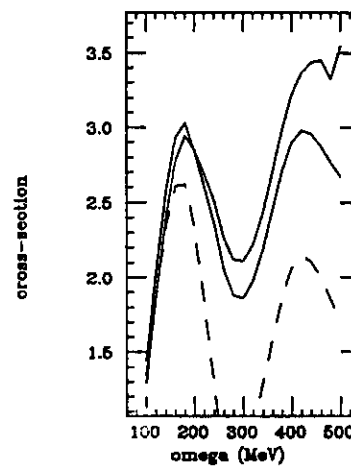
$E_0 = 600.0$ MeV, $\theta = 40.0$ deg



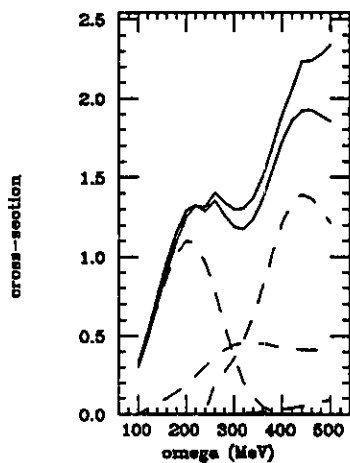
$E_0 = 600.0$ MeV, $\theta = 50.0$ deg



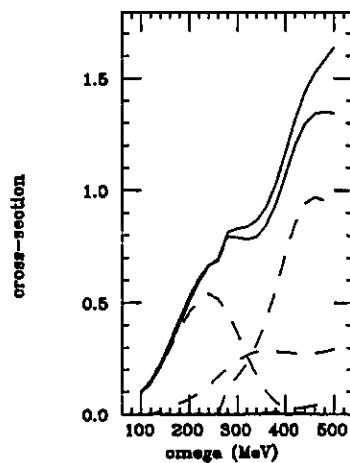
$E_0 = 600.0$ MeV, $\theta = 60.0$ deg



$E_0 = 600.0$ MeV, $\theta = 70.0$ deg



$E_0 = 600.0$ MeV, $\theta = 80.0$ deg



$E_0 = 600.0$ MeV, $\theta = 90.0$ deg

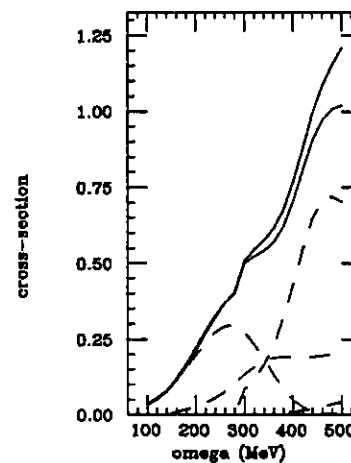
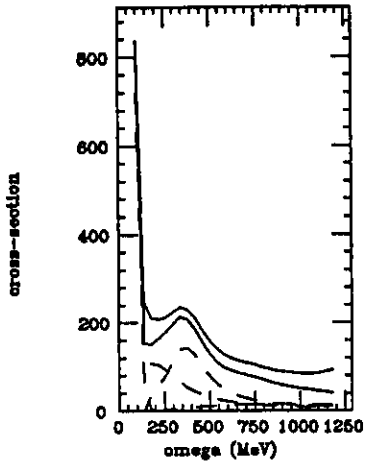
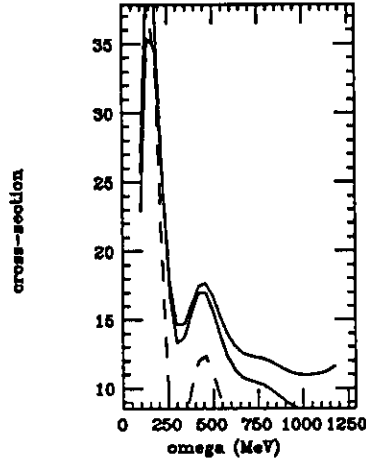


Figure 11. $E_0 = 600$ MeV CLAS cross-sections (nb/MeV-sr). Elastic radiative tail included.

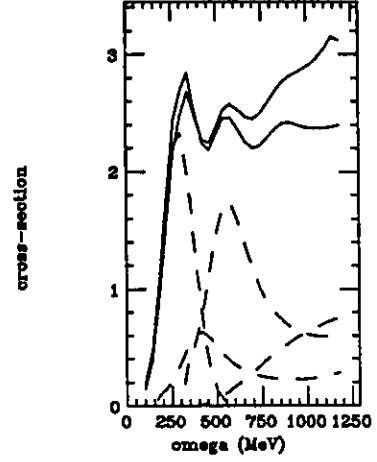
$E_0=1500.0$ MeV, $\theta= 10.0$ deg



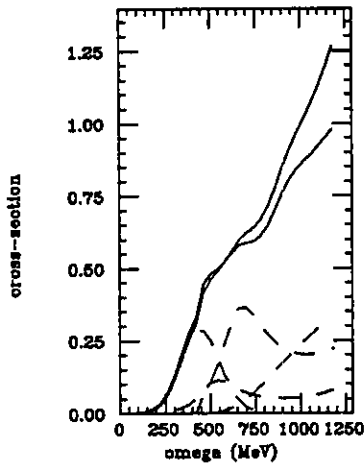
$E_0=1500.0$ MeV, $\theta= 20.0$ deg



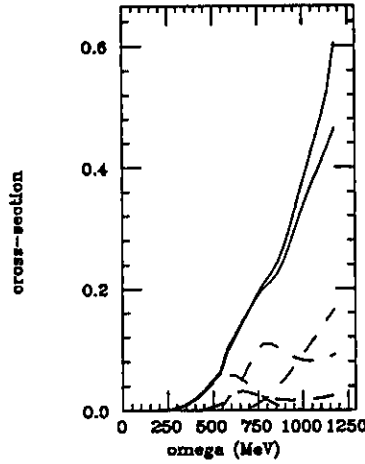
$E_0=1500.0$ MeV, $\theta= 30.0$ deg



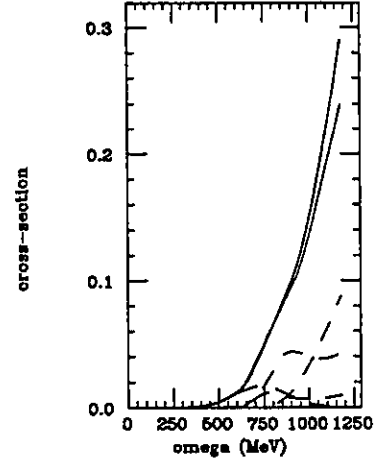
$E_0=1500.0$ MeV, $\theta= 40.0$ deg



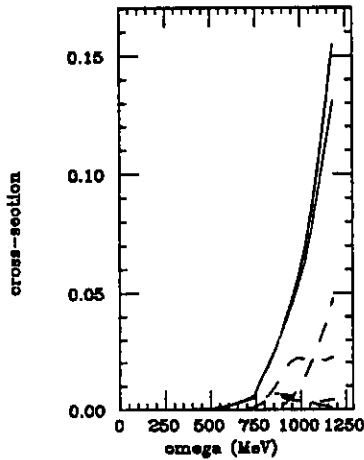
$E_0=1500.0$ MeV, $\theta= 50.0$ deg



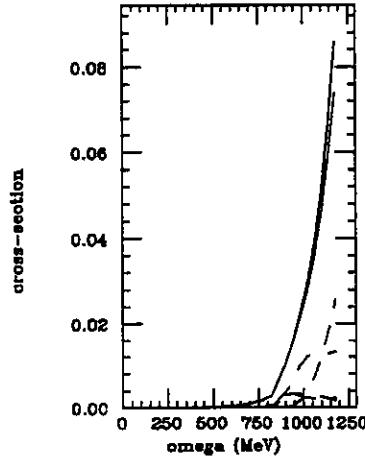
$E_0=1500.0$ MeV, $\theta= 60.0$ deg



$E_0=1500.0$ MeV, $\theta= 70.0$ deg



$E_0=1500.0$ MeV, $\theta= 80.0$ deg



$E_0=1500.0$ MeV, $\theta= 90.0$ deg

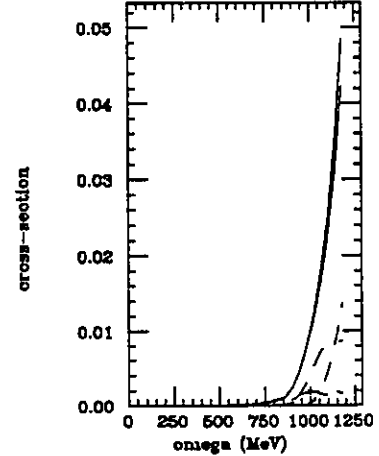


Figure 12. $E_0 = 1500$ MeV CLAS cross-sections (nb/MeV-sr). Elastic radiative tail included.

Variable	Bin Size	Number of Bins
θ_e	10°	9
ω	30–60 MeV	20
ϵ_m	10–40 MeV	30
θ_{pq}	20°	6
ϕ_{pq}	90°	4
Total		$1 \cdot 10^5$

Table 1. Data Binning

kinematic regime (eg: quasielastic). We will bin the missing energy spectrum data into 10 MeV bins in the single particle excitation region and 40 MeV bins beyond that region. We plan to bin the data according to the angle between the proton and the momentum transfer, θ_{pq} , in 20° bins. This might be too large. We will bin the data according to the azimuthal angle between the proton and the momentum transfer, ϕ_{pq} , into four bins. These bins might also be too large. Thus, there will be a total of approximately $1 \cdot 10^5$ bins. If we want 500 events per bin and we assume a 50% efficiency to detect secondary particles, then we need $1 \cdot 10^8$ events. At 300 events per second, this will take 100 hours per beam energy. This assumes that the trigger is efficient enough that only ‘interesting’ events are acquired and that different ‘interesting’ events with different cross-sections are acquired at the same rate. To achieve this goal, we will require electron identification in the trigger over a very large range of angles. A less efficient trigger will reduce the available statistical precision.

At each energy, we will use a Hydrogen target for normalization. This will allow us to absolutely normalize the electron detection efficiency using the known $^1\text{H}(e,e')$ cross-section and to absolutely normalize the proton detection efficiency using the ratio $^1\text{H}(e,e')/^1\text{H}(e,e'p)$. Since the $^1\text{H}(e,e'p)$ reaction is kinematically overdetermined, we will also use it to determine the CLAS angle and momentum measurement accuracies. Similarly, we can use the $\text{H}(e,ee'p\pi)$ reaction to determine pion detection and identification efficiencies. We will use the $\text{D}(e,e'pn)$ reaction to determine the absolute neutron detection and identification efficiencies. We will need 12 hours at each beam energy for Hydrogen normalization.

If the data acquisition rate is 300 events per second, then we will need 100 hours per target per beam energy. For five targets at four different beam energies, we will need 2000 hours of beam time. We also want 100 hours at each beam energy (400

hours total) to investigate one target in more detail. Thus, we are asking for 2450 hours.

If the data acquisition rate is 100 events per second, then we will either need more beam time, use fewer targets, or take less statistics.

2450 hours of beam time will allow us to characterize the electron scattering reaction mechanisms over a very wide range of targets and kinematics. However, this beam time will be sufficient only for an initial survey experiment. The statistics will be high enough to give us an overview of the reaction mechanisms involved in electron scattering. They will not be enough to make detailed studies of specific reaction mechanisms and they will also not be enough to make high precision response function separations.

IV. Conclusion

This experiment is the simplest possible electron scattering experiment using the CLAS. We will be using as loose a trigger as possible and studying all final states. We will not need a photon tagger, complex triggering schemes, or sophisticated targets. This experiment will gather data about the performance of the CLAS with electron beams and also about the (e,e') response that will be needed to plan later, more in-depth, studies. It will make an ideal commissioning experiment for the CLAS.

The scope of CLAS experiments is much greater than that of any done before in nuclear physics. In effect, many experiments are performed simultaneously and, in order to accumulate enough statistics for each 'experiment', large amounts of accelerator time are required.

The work we propose will allow us to characterize the $(e,e'p)$ reaction over a very wide range of momentum transfer and reaction mechanism for several representative nuclei and will provide good commissioning experiments for use of the CLAS with electron beams.

Collaborators for these experiments will involve groups from several universities. The collaboration is expected to grow to match the wide range of physics expected from these measurements and the concomitant experimental demands.

REFERENCES

- [1] G. van der Steenhoven *et alia*, *Nucl Phys A* **480**, 547 (1988).
- [2] P.E. Ulmer *et alia*, *Phys Rev Lett* **61**, 2001 (1988).
- [3] J.W.A. den Herder *et alia*, *Nucl Phys A* **490** (1988) 507.
- [4] L. Weinstein *et alia*, PhD Thesis, MIT (1988) and *submitted to Phys Rev Lett*; J. Morrison, MIT, *private communication*.
- [5] P.E. Ulmer *et alia*, *Phys. Rev. Lett.* **59**, 2259 (1987)
- [6] P. Barreau *et alia*, *Nucl Phys A* **402**, 515 (1983).
- [7] J.M. Finn, R.W. Lourie and B.H. Cottman, *Phys Rev* **C29**, 2230 (1984).
- [8] P.E. Ulmer *et alia*, *Phys Rev Lett* **59**, 2259 (1987).
- [9] R.W. Lourie *et alia*, *Phys. Rev. Lett.* **56**, 2364 (1986)
- [10] J.M. Laget, *private communication*.
- [11] T. Takaki, *Phys Rev Lett* **62** (1989) 395.
- [12] H. Baghaei *et alia*, *Phys Rev* **C39** (1989) 177
- [13] M. Kanazawa *et alia*, *Phys Rev* **C35**, 1828 (1987).

Continuous Electron Beam Accelerator Facility

12000 Jefferson Avenue
Newport News, Virginia 23606
(804) 249-7100

Proposal Number: PR-89-027

Proposal Title: Coincidence Reaction Studies with the LAS

Spokespersons/Contact Persons: W. Bertozzi, W. Boeglin, L. Weinstein

Proposal Status at CEBAF:

Conditional approval. The overlap of proposals PR-89-015, -017, -027, -031, -032, and -036 is high but not complete. The proponents should attempt to coordinate beam energies, targets, and data acquisition, so that the six experiments can run simultaneously. The present feeling of the PAC is that the initial measurements should be limited to ^3He and one heavy nucleus, ^3He having priority, and that the optimal beam energies and kinematics are close to those in PR-89-031.



John Dirk Walecka
Scientific Director